Aqueous gelcasting of CeO_2 ceramics using water-soluble epoxide

Séverin Chaigne, Gaëlle Bœuf-Muraille, Rémy Boulesteix, Alexandre Maître, Bénédicte Arab-Chapelet, Thibaud Delahaye

Aqueous gelcasting of CeO_2 ceramics using water-soluble epoxide

Séverin Chaigne[1,2], Gaëlle Bœuf-Muraille[1], Rémy Boulesteix[1], Alexandre Maître[1], Bénédicte Arab-Chapelet[2], Thibaud Delahaye[2]

[1] Univ. Limoges, CNRS, IRCER, UMR 7315, F-87000 Limoges, France

[2] CEA, Nuclear Energy Division, Research Department on Mining and Fuel Recycling Process, SFMA/LPCA, Marcoule, F-30207 Bagnols-sur-Cèze, France

Corresponding author

Dr. Rémy Boulesteix

E-mail: remy.boulesteix@unilim.fr

Postal address: IRCER, 12 rue Atlantis 87068 Limoges

Abstract:

Manufacturing of CeO_2 ceramics by an aqueous gelcasting shaping process was studied. This study has focused on the identification of critical parameters that influence the properties of suspensions and CeO_2 ceramics. It is shown that ethylene glycol diglycidyl ether (EGDGE) and 3,3-diaminodipropylamine (DPTA) are suitable gelling agents for gelcasting process. This system has many advantages as low toxicity, limited impact on

suspensions viscosity, and it does not disturb CeO_2 dispersion by ammonium polyacrylate (PAA) in water. As a result, suspensions with high solid loading of 50 vol.% were obtained. Solid loading appears as a critical parameter to control suspensions rheology, casting feasibility and final microstructural features of CeO_2 ceramics. Finally, CeO_2 ceramics with high relative density (> 96%), good surface finish and complex **shape** were manufactured by gelcasting and natural sintering at 1500°C for 1 h.

Keywords: Gelcasting; EGDGE; CeO_2; ceramics; colloidal suspensions.

1. Introduction

Gelcasting is an attractive near-net-shape shaping method of advanced ceramic materials. It has been first developed at Oak Ridge National Laboratory (ORNL, USA) by Omatete and Janney during 90's decade [1,2]. This method is presented in Figure 1. In this process, ceramic slurry is casted into a non-porous mold. It turns to solid powder compacts that can be demolded and handled thanks to a gelation process induced by a chemical reaction. After reaction, ceramic particles are trapped into a macromolecular organic network. Green compacts can be then dried and heated at moderated temperatures, usually lower than 800°C, in order to remove solvent and organic residues by thermolysis. Final sintering can be then conducted to densify the material until the desired microstructural features. Gelcasting process enables the manufacturing of high quality and complex shaped ceramics with a low proportion of organic compounds (*i.e.* < 4wt.%) [3]. Different chemical compounds are usually used: a monomer as repeat unit of the polymer gel, a cross-linker that branches the long chains of polymer, an initiator as catalyzer of the reaction and a dispersant to avoid the aggregation of the particles in the suspension. First gelcasting experiments were lead on Al_2O_3 powder and have used the free radical **polymerization** of acrylamide monomer as gelling agent [4]. Nevertheless, acrylamide was found to be neurotoxic and research was rapidly orientated to low toxic monomers [5,6] or nontoxic gelling system [7] for industrial applications. As an alternative to free-radical chemistry in the acrylamide or acrylate **polymerization**, polyaddition based on the reaction between an epoxide and an amine hardener has been then developed. The first epoxide system used to elaborate alumina ceramics was the sorbitol polyglycidyl ether (SPGE) [8,9]. This compound forms polymer via a nucleophilic addition reaction that is not affected by oxygen. The reaction

can therefore be conducted under air atmosphere. Because of some disadvantages like high viscosity and low water solubility (*i.e.* < 10 wt.%), new epoxide molecules were investigated like ethylene glycol diglycidyl ether (EGDGE), polyethylene glycol diglycidyl ether (PEGDGE), glycerol polyglycidyl ether (GPGE) or resorcinol diglycidyl ether RDGE [8,9]. Among these four gelling agents, EGDGE was found to be the most suitable for the gelcasting of alumina ceramics, owing to its high solubility in water, low viscosity of obtained suspensions as well as the high strength of the green bodies [10,11]. Nevertheless, interactions of the different chemical compounds involved in the gelcasting process remain unclear. In particular, interaction between gelling agents and dispersant **was** not previously investigated.

Moreover, the influence of main process parameters (organic additives content, solid loading, viscosity, etc.) needs to be better understood to control the final properties **(*e.g.* relative density, shape, mechanical properties)** of the ceramics parts manufactured by gelcasting. **The main challenge generally rely on the difficulty of obtaining ceramic parts with homogeneous and dense microstructure and with limited deformations after sintering. This strongly depends on suspensions characteristics that should be: homogeneous, low viscous, stable, and highly concentrated to ensure good particles packing in green parts. If this is not the case, the presence of powder agglomerates and/or large pores will perturb the densification process, *i.e.* differential sintering will occur leading to inhomogeneous and porous ceramic material at the end of the fabrication process** [12]**. Moreover, the lower is the loading charge of suspensions, the higher should be the shrinkage and deformations during sintering.**

In this study, the manufacturing of cerium (IV) oxide CeO_2 ceramics was investigated by the gelcasting method using EGDGE and dipropylenetriamine (DPTA) as hardener. CeO_2 is widely used for electrolyte materials in the intermediate temperature solid oxide fuels cells (IT-SOFCs) [13–15], for automotive catalysts [16–18], for the oxygen storage [19], for optical applications [20,21] and as a non-radioactive surrogate of actinide oxides in nuclear fuel fabrication studies [22–24]. **For all of these applications, various shapes and microstructure (*e.g.* controlled porosity and grain size) are needed. Thus, the aim of this work is to demonstrate the feasibility of CeO_2 ceramics with dense microstructure (*i.e.* relative density higher than 96%) and complex shape (ball, lens, tube, etc.) by a near-net shape gelcasting process. More specifically. the** influence of the addition of EGDGE and **PAA** on the properties CeO_2 ceramics was investigated at each process step: (i) aqueous suspensions properties (rheological, gelling kinetics, etc.), (ii) green compacts microstructure and (iii) its evolution during thermal treatment. Finally, the manufacturing of CeO_2 ceramics with dense, homogeneous microstructure and **controlled** shape **will be** demonstrated.

2. Experimental procedure

2.1. Manufacturing process of CeO_2 ceramics

First, aqueous suspensions of CeO_2 powder added with gelling agents were manufactured as follow: CeO_2 powder (Opaline^{TM}, A.M.P.E.R.E Industry, France) was added to EGDGE (Tokyo Chemical Industry CO, LTD, Tokyo, Japan) and PAA (Darvan® 821A, Vanderbilt Minerals, LLC, Norwalk, USA) diluted in distilled water at room temperature. The quantity of PAA was varied between 0.35 wt.% and 1 wt.%. After homogenization, 0.250 mL of 3,3-diaminodipropylamine (DPTA, Tokyo

Chemical Industry Co., LTD, Tokyo, Japan) per gram of EGDGE was added to the suspension. The obtained slurry was poured in a non-porous mold and then moved into an oven at 50°C for 12 h. The obtained green parts after gelation were dried and calcined under air at 650°C for 1 h with a heating rate of 0.5°C.min^{-1}. Sintering was finally conducted under air atmosphere at various temperatures during 1 h with a heating rate of 5°C.min^{-1}.

2.2. Characterizations

The powder was analyzed by laser granulometry (Partica LA950, Horiba, Japan) and specific surface area (S_{BET}) measurement (ASAP 2020, Micromeritics, USA). Chemical analysis by glow discharge mass spectrometry (GDMS, EAG Labs, France) and transmission electron microscopy (TEM, JEOL 2100F, France) were also performed.

Zeta potential measurements were performed on different CeO_2 suspensions loaded with 1 wt.% of ceria powder with an acoustosizer (IIS^{TM}, Colloidal Dynamics, LLC, USA). The pH was adjusted by adding 0.1 M solutions of HCl or NaOH to decrease or increase the pH, respectively.

The rheological behavior of concentrated suspensions was studied by measuring the apparent viscosity using rotational rheometer (Haake Mars III, ThermoFisher Scientific, USA) within the shear rate range of 0.1-1000 s^{-1} using plate (35 mm, gap 1 mm) measuring configuration. Gelation kinetics of suspensions were also evaluated by varying the temperature under oscillation mode (shear rate = 0.1 s^{-1}).

Scanning electron microscopy (SEM) was conducted on a frozen suspension and compared to corresponding green compacts after gelation. Observations were conducted using an ESEM instrument Quanta^{TM} 450 FEG (FEI, Czech Republic) with the Gaseous

Secondary Electron Detector (GSED). **Observations were** operated in low vacuum conditions with a pressure fixed at 400 Pa for the frozen suspension and varies between 100 Pa and 120 Pa for the green compact. The frozen suspension sample was prepared as follow: one droplet of suspension was deposited on a flat specimen carrier (1.2 mm of diameter). The specimen carrier was then frozen in liquid nitrogen at a rate of about 9000°C.s^{-1} under a pressure of 1910 bars with a high-pressure freezer (Leica EMPACT, Leica Microsystems, Vienna, Austria). Then, the sample was kept in liquid nitrogen until it was placed in the ESEM for observation. A Peltier cooled sample holder was used to maintain the sample at a low temperature during the analysis.

Thermal behaviour of green parts obtained after gelation and drying was studied by thermogravimetry analysis (TG/DSC Netzsch STA449 F3 Jupiter®, Germany) under air atmosphere at 1000°C with heating rate of 5°C.min^{-1}. Linear shrinkage during pressure-less sintering under air was followed by a thermo-mechanical **analyzer** (TMA Setsys evolution, Setaram, France) with a heating rate of 10°C.min^{-1} until 1700°C. Samples obtained by gelcasting were sintered at 1500°C for 1 h with a heating rate of 5°C.min^{-1}.

After thermal treatments, relative density of samples was determined using Archimedes method in ethanol. Before microstructural observations, sintered samples were previously polished with SiC grinding paper and 0.1 µm alumina suspension and thermally etched under air atmosphere during 30 minutes at temperatures lower than sintering temperature by 100°C. Conventional SEM (IT300 JEOL, Japan) was used to observe samples microstructure. The grain size was determined by the intercept method using ImageJ software (« *Image Processing and Analysis in Java* », National Institutes of Health, Etats-Unis).

3. Results and discussion

3.1. Study of aqueous suspensions

First, commercial ceria powder CeO_2 was characterized. The powder was **analyzed** by laser granulometry, specific surface area (S_{BET}) measurement, chemical analysis by glow discharge mass spectrometry (GDMS) and transmission electron microscopy (TEM). The results of laser granulometry analyses gives d_{50} of 0.085 µm. This value is in good agreement with the grain sizes observed on TEM images (Figure 2). Also is visible on Figure 2 that CeO_2 particles appear well **crystallized** with isotropic shape. The specific surface area is 4.7 $m^2.g^{-1}$ and chemical purity measured by GDMS was found to be higher than 99.8% by weight. From all of these results, CeO_2 commercial powder appears chemically pure, well **crystallized** and deagglomerated with a mean particle size close to 85 nm.

The influence of the addition of EGDGE on the rheological properties of the CeO_2 suspensions was investigated. A low viscosity is necessary for the casting of ceramic slurry and the influence of gelling agents on the viscosity of the suspensions is a critical parameter in gelcasting process. The viscosity of 30 vol.% CeO_2 aqueous suspensions with or without EGDGE and at different concentrations of PAA was measured at a fixed shear rate of 97 s^{-1} and reported in Figure 3a. The viscosity of the **suspension** without EGDGE is almost a plateau but a slight increase of viscosity can be noticed around the value of 0.50 wt.% of PAA. PAA is a weak polyelectrolyte that ionizes in water according to Eq.(1) and Eq.(2):

$$RCOONH_4 = RCOO^- + NH4^+ \qquad (eq.1)$$

$$RCOO^- + H^+ = RCOOH \qquad (eq.2)$$

Consequently, the dissociation rate of PAA depends on the pH of the **suspension**. In appropriate pH conditions, the carboxylate groups can be adsorbed onto particles surface. Their presence introduces electrostatic and steric repulsions that will compensate the attractive van der Waals forces [25]. That will lead to less aggregation of the particles and so to a lower viscosity of the suspensions. A minimum of viscosity is reached when the amount of PAA is sufficient to stabilize most of the particles in the suspension. Above this value, the viscosity slightly increases because of an over-saturated adsorption of PAA at the particles surface. In such case, PAA in excess remains in solution increasing the ionic force that tends to increase the viscosity [26]. The viscosity of the suspension with EGDGE is much more affected by PAA content (Figure 3a). A strong increase of viscosity is observed on each side of the same value of 0.50 wt.% of PAA, especially for lower content of PAA. As the rheological behaviour and corresponding viscosity are the same for 0.5 wt.% of PAA (Figure 3b), strong increasing of viscosity in presence of EGDGE should be explained by a competition between PAA and EGDGE for adsorption at CeO_2 surface. It must be noticed that the natural pH of the suspension containing CeO_2, EGDGE and PAA is 4.6. In these conditions, epoxide functions of EGDGE molecule can be hydrolyzed leading to the formation of hydroxyl groups that can be adsorbed onto the surface of CeO_2 particles. As no significant electrical charge is added by EGDGE adsorption, viscosity would increase by branching effect between CeO_2 particles. When PAA concentration increases to the optimum value of 0.5 wt.%, it should gradually replace EGDGE at the surface of CeO_2 particles leading to strong viscosity decreasing. Interestingly, the addition of EGDGE does not influence the optimal amount of PAA needed to **stabilize** the particles. This means that PAA carboxylate groups should be stronger than hydroxyl

groups of **hydrolyzed** EGDGE to adsorb on CeO_2 surface. As a result, the addition of 0.5 wt.% of PAA allows **obtaining** suspensions with a low viscosity with or without EGDGE addition. Moreover, shear thinning fluid (non-Newtonian fluid) with low value of the viscosity, typically less than 1.5 Pa.s for a shear rate of 20 s^{-1} [27], as observed in Figure 3b ensures suitable conditions for casting process.

Then, the zeta potential (ξ) of CeO_2 suspensions was investigated under a large range of pH (*i.e.* 2 < pH < 12) and the influence of EGDGE addition has been considered (Figure 4). **On one hand, it should be noticed that the natural pH of CeO_2 suspensions was stable with time (pH around 5-7 depending on PAA and/or EGDGE addition). The conductivity of suspensions was also stable with time and its variations remain very limited in a large pH range (*i.e.* conductivity lower than 0.5 mS.cm^{-1} for 3 < pH < 11 for all analyzed suspensions). Moreover, spontaneous gelation, *i.e.* without addition of initiator/catalyzer in the suspensions, was never observed. Thus, spontaneous CeO_2 hydrolysis in water was not expected to occur in our conditions. On the other hand,** the zeta potential of CeO_2 aqueous suspension continuously decreases with increasing pH. The isoelectric point (IEP, *i.e.* pH for ξ = 0 mV) of pure CeO_2 **is** around pH = 7.6. This latter result is in accordance with reported values in the literature [28]. As most of oxides, the charge surface of the CeO_2 particles in water is governed by the adsorption or desorption of protons (H^+) leading to Eq.(3) and Eq.(4) in water:

$$Ce-OH + H_2O \leftrightarrow Ce-OH_2^+ + OH^- \quad for\ pH < IEP \qquad (eq.\ 3)$$

$$Ce-OH + H_2O \leftrightarrow Ce-O^- + H_3O^+ \quad for\ pH > IEP \qquad (eq.\ 4)$$

According to these equations, by increasing the pH the surface charge of CeO_2 goes from positive for pH lower to IEP to negative for pH higher than IEP. From Figure 4,

CeO_2 also shows relatively low absolute values of zeta potential in pure water (< 20 mV) that is too low to ensure good dispersion. PAA addition leads to a strong decrease of the zeta potential that reaches high negative values (*i.e.* ξ < -40 mV for pH > 4). Also, IEP is strongly shifted to low values of pH (IEP = 2), putting in evidence the anionic nature of this compound and its relevancy to be used as a common dispersing agent. For a pH between 2 and 4, the zeta potential of CeO_2 suspension containing PAA strongly decreases, then it decreases more slowly until 10 and decreases again faster for pH > 10. Thus, PAA induces highly negative zeta potential at the surface of CeO_2 particles over the whole range of pH studied. At pH > 10, the decrease of zeta potential values can be explained by the disappearance of ammonium cation NH_4^+ that participates to the neutralization of the negative charges along the chains of PAA. Indeed, the pK_a constant of the NH_4^+/NH_3 couple is 9.25, so above this value of pH the concentration of NH_4^+ decreases in favor to NH_3.

The addition of EGDGE to CeO_2 + PAA suspensions results in a small increase of zeta potential. Nevertheless, the whole trend of zeta potential curve is similar to the suspension without EGDGE. That confirms the slight cationic character of EGDGE which is concordant with the literature [29]. As a result, PAA adsorption should stay the predominant phenomenon occurring for the stabilization of the particles whereas EGDGE should be only slightly adsorbed. This result is in accordance with other studies lead on other ceramic aqueous colloidal suspensions like lead zirconate titanate [30] or silica, zirconia, alumina [29] containing ammonium poly(methacrylate) as dispersant and EGDGE as gelling agent. From these results, EGDGE appears to be almost neutral in CeO_2 aqueous suspensions containing suitable amount of PAA (*i.e.* 0.5

wt.%). The **elaboration** of concentrated suspensions of CeO_2 containing EGDGE as gelling agent can be thus envisaged.

3.2. Study of gelation kinetics

This paragraph is devoted to the study of gelling kinetics of CeO_2 suspensions. Investigated parameters were the temperature and solid loading. Gelation kinetics were studied thanks to the measurement of *idle time* method, *i.e.* the measurement of the characteristic time for the beginning of **polymerization** reaction. This time corresponds to the period for primary reactions between the monomer and initiator/catalyst/amine hardener to take place. Idle time can be assumed to be inversely proportional to the reaction rate, thus it may be expressed by an Arrhenius-type equation [31]:

$$t_{idle} \propto \frac{1}{r} = A\exp\left(\frac{E_a}{RT}\right) \qquad (eq.5)$$

where r is the reaction rate, A a constant, R the gas constant and E_a the activation energy of **polymerization** reaction. It can be measured from rheological behaviour analysis, especially from curves representing the viscosity as a function of time. In practice the first and second part of the curve (corresponding to a stable viscosity and then a rapid increasing of the viscosity, respectively) are fitted by straight lines and t_{idle} corresponds to the time at intersection of these lines [11].

Figure 5a shows the variation of concentrated ceria suspensions viscosity at different temperatures with a fixed DPTA concentration (0.250 mL per gram of EGDGE) and a fixed solid loading of CeO_2 (30 vol.%). For each curve, corresponding to different temperatures, the viscosity remains very low until a certain time and then rapidly increases. As expected, the reaction rate is higher when the temperature is increased,

going from approximately 8 min at 55°C to 66 min at 25°C for suspensions loaded with 30 vol.% of CeO_2. The idle time can be determined based on these curves as illustrated in Figure 5b. As a result, Arrhenius plot can be drawn over the **whole temperature** range (Figure 5c). Similar analyses were conducted with suspensions containing different amount of CeO_2 to determine the influence of solid loading on gelation kinetics. The gelation of suspensions with CeO_2 volume loadings from 0% (pure EGDGE + DPTA aqueous solution) to 40% was followed by the same procedure. The analysis on more concentrated suspensions did not give relevant results because suspensions were too viscous. Arrhenius plot of the idle time versus inverse of temperature for different solid loading is given in Figure 5d. First, it can be noticed that all plots can be fitted with a linear equation and are thus in accordance with Eq. 5. Corresponding values of activation energy were noticed in Table 1. Figure 5d shows that the increasing of solid loading tends to slightly increase the gelation kinetics at a given temperature. Moreover, activation energy for gelation is very similar between ceria suspensions and powder-free sample. Thus, the gelation process should be controlled by the same rate-limiting reaction mechanism for all investigated formulations and temperatures. As a result, CeO_2 particles should have a branching effect between monomer and polymer entities during the **polymerization** reaction that tends to increase its rate, but reaction mechanisms should not be affected by CeO_2 incorporation. The use of thermosetting resin like EGDGE + DPTA system in ceramics suspensions thus allows a good control of suspensions viscosity and of their gelation time via the monitoring of the temperature.

3.3. Thermal behavior of green compacts

At first, CeO_2 suspensions with two solid loading (*i.e.* 20 vol. % and 47 vol. %) were observed by SEM at -10°C under vacuum after high pressure freezing technique. Such technique allows freezing suspensions at a very high rate that ensures to observe particles in similar arrangement than in the liquid [32]. Comparison between Figure 6a and Figure 6b shows that **an increase of** solid loading allows obtaining more homogeneous distribution of CeO_2 particles with less voids. The suspension with 47 vol.% of CeO_2 shows a more regular, almost homogeneous microstructure with particles very close together, whereas the microstructure of the suspension with 20 wt.% of CeO_2 is rather inhomogeneous with voids between small agglomerates of particles. The mean size of these voids is in the order of one micrometer, much larger than CeO_2 particles diameter. For the suspension with 47 vol.% of CeO_2, the microstructure is preserved during drying and debinding as illustrated in Figure 6c. As a result, the pore size distribution obtained by mercury porosimetry in Figure 6d is very homogeneous with a diameter in the same order of magnitude than CeO_2 particles (*i.e.* 112 nm). **These analyses show** that gelcasting allows keeping a good homogeneity from liquid (suspensions) to solid (green compacts). **These results also highlight the effect of solid-loading on green compacts microstructure that is more homogeneous and more compact when suspensions are well dispersed, low viscous and highly concentrated.**

Then, thermogravimetry (TG) analyses coupled with differential scanning calorimetry (DSC) were performed on a CeO_2 green compact from a 47 vol.% suspension. TG curve shown in Figure 7a presents two main mass losses with a first loss at 130°C which corresponds to the **vaporization** of the adsorbed water and a second between 200°C and 450°C related to the removal of organics (polymer and dispersant). In fact, this later

mass loss of about 3.7 wt.% is in accordance with calculated mass of organics for such formulation (*i.e.* 3.6 wt.%). This mass loss is strongly exothermic as it is shown by the DSC curve. The thermal degradation of organics should correspond to an oxidization rather than simple pyrolysis that is often endothermic. As a result, thermal debinding must be performed at a very slow heating rate (< 1°C/min) under air to avoid uncontrolled and damaging combustion of organics. Slow heating rate will also allow a complete removal of all gaseous species resulting from organics thermal degradation.

Sintering behavior of CeO_2 green compacts obtained from a 47 vol.% CeO_2 suspension was then evaluated by dilatometric analysis under air at 10°C.min^{-1}. The linear shrinkage and linear shrinkage rate versus temperature are shown in Figure 7b. Below 900°C the linear shrinkage increases slowly and the linear shrinkage rate remains constant because of simple thermal expansion. Between 900°C and 1600°C, strong shrinkage due to the densification is registered. The maximum densification rate is reached at 1340°C. This result shows that the densification of CeO_2 compacts starts around 1000°C, which is a relatively low temperature comparing to common sintering temperatures reported for CeO_2 ceramics. Low sintering temperature is generally observed for green compacts manufactured from fine and reactive powders and with high microstructural homogeneity [12]. Sintering temperature can be decreased by several tens of degrees in such favorable conditions. **Figure 7b also shows that densification is almost finished at 1500°C. Therefore, this temperature will be used for CeO_2 sintering tests in the next part of the study.**

3.4. Influence of solid loading

Several parameters needs to be controlled during all process steps in order to manufacture defect-free ceramics. Especially, a lot of solvent and organics need to be

eliminated from the green pieces. As a consequence, drying and debinding must be as slow as possible in order to avoid cracks. Also, a good solution to limit cracks appearance is to increase solid-loading. There is thus a compromise between suspensions solid-loading, that should be as high as possible to limit cracks, and suspensions viscosity, that should be as low as possible to ensure good casting. Samples from CeO_2 suspensions with solid-loading ranging from 20 vol.% to 50 vol.% were manufactured. After casting into a non-porous mold, samples were placed in an oven at 50°C to accelerate the gelation reaction. After 12 h, as-obtained green compacts were sufficiently hard to be easily unmolded and manipulated. Samples were then dried, debinded and finally sintered at 1500°C during 1 h under air atmosphere with a heating rate of $5°C.min^{-1}$.

Table 2 presents the influence of the solid loading on the relative density of green compacts. As expected the higher is the solid loading, the higher is the relative density. The relative density of **dried** green bodies varies from 48.1 to 55.3% when the solid-loading increases from 20 vol.% to 50 vol.%. Corresponding view of green samples is reported in Figure 8a. It shows that some macroscopic defects are visible on samples, especially for low or high solid loading (*i.e.* ≤ 30 vol.% and ≥ 50 vol.%, respectively). As expected, samples with such low solid loading undergo strong deformation owing to high level of shrinkage. **The shrinkage was measured at different steps of the thermal treatment (*i.e.* after drying, debinding and sintering) and for different solid-loading. The data are reported in Figure 8b.** Shrinkage during drying and debinding steps continuously decreases when solid loading increases. Such behaviour can be explained by CeO_2 particles rearrangement when solvent (water) and organics are removed. For solid loading ≥ 47 vol. %, a minimum of shrinkage is observed prior

to sintering meaning that sufficiently high compacity is reached to avoid such microstructural rearrangement.

After sintering, each sample was observed by SEM as exposed in Figure 9. The corresponding grain size and relative density were also reported in Table 2. The grain size varies between 2.65 µm and 4.10 µm and the **relative** density of sintered parts **increases** from 84.4% to 96.1% **when the solid-loading increases from 20 vol.% to 50 vol.%.**

CeO_2 sample obtained from 20 vol.% suspensions presents a very heterogeneous microstructure with porous and dense areas. This result is probably due to differential shrinkage from non-homogeneous particles packing in the green body. By increasing the solid loading, the microstructure appears to be more homogeneous and denser with slightly higher grain size. Solid loading of 47 vol.% and 50 vol.% lead to similar relative density and grain size after sintering. This behaviour is in accordance with Figure 8b showing that shrinkage is very similar during the overall thermal treatment for these samples. From these results, a solid loading of 47 vol.% seems to be well adapted for CeO_2 ceramics manufacturing by gelcasting and natural sintering.

Finally, CeO_2 ceramics were shaped in different forms by gelcasting: sphere, hollow cylinder and **lens** then sintered at 1500°C for 1 h. CeO_2 ceramics with well-controlled dimensions and good surface finish without any polishing or rectification were obtained (Figure 10). This **last** result shows that gelcasting can be a suitable shaping process for near net shape manufacturing of **CeO_2** ceramics.

4. Conclusion

Gelcasting of CeO_2 aqueous suspensions in presence of EGDGE + DPTA was investigated in this study. Conclusions can be summarized as follow:

First, rheological and zetametry measurements have demonstrated that concentrated, stable and well-dispersed CeO_2 suspensions can be obtained for pH > 5 with 0.5 wt.% of PAA as dispersant. Especially, this study has shown that the incorporation of gelling agents does not disturb the action of dispersant, probably because of preferential adsorption of PAA in regards to EGDGE on CeO_2 particles surface.

Second, study of gelation kinetics has shown that **polymerization** reactions should be controlled by the same rate-limiting reaction mechanism with activation energy of about 60±5 $kJ.mol^{-1}$. Slight positive effect on gelation kinetics of solid loading was also registered, **probably owing to branching effect of CeO_2 particles**.

Finally, the solid loading of suspensions has appeared to be a critical parameter for the control of microstructure and shape of CeO_2 ceramics. Suspensions with a solid loading equal to 47 vol.% **is** a good compromise **to obtain samples with good quality**. As a result, CeO_2 ceramics with high relative density (> 96%), good surface finish and complex shape can be manufactured by gelcasting and natural sintering at **only** 1500°C for 1 h.

Acknowledgements

This work was funded by the French National Research Agency within the A.S.T.U.T.E project (contract Nb ANR-15-CE08-0011-03).

References

[1] M.A. Janney, O.O. Omatete, Method for molding ceramic powders using a water-based gel casting, US5028362 A, 1991.

[2] M.A. Janney, O.O. Omatete, Method for molding ceramic powders using a water-based gel casting process, US5145908 A, 1992.

[3] R. Gilissen, J.P. Erauw, A. Smolders, E. Vanswijgenhoven, J. Luyten, Gelcasting, a near net shape technique, Mater. Des. 21 (2000) 251–257. doi:10.1016/S0261-3069(99)00075-8.

[4] A.C. Young, O.O. Omatete, M.A. Janney, P.A. Menchhofer, Gelcasting of Alumina, J. Am. Ceram. Soc. 74 (1991) 612–618. doi:10.1111/j.1151-2916.1991.tb04068.x.

[5] O.O. Omatete, M.A. Janney, S.D. Nunn, Gelcasting: From laboratory development toward industrial production, J. Eur. Ceram. Soc. 17 (1997) 407–413. doi:10.1016/S0955-2219(96)00147-1.

[6] M.A. Janney, O.O. Omatete, C.A. Walls, S.D. Nunn, R.J. Ogle, G. Westmoreland, Development of Low-Toxicity Gelcasting Systems, J. Am. Ceram. Soc. 81 (1998) 581–591. doi:10.1111/j.1151-2916.1998.tb02377.x.

[7] J. Yang, J. Yu, Y. Huang, Recent developments in gelcasting of ceramics, J. Eur. Ceram. Soc. 31 (2011) 2569–2591. doi:10.1016/j.jeurceramsoc.2010.12.035.

[8] X. Mao, S. Shimai, M. Dong, S. Wang, Gelcasting of alumina using epoxy resin as a gelling agent, J. Am. Ceram. Soc. 90 (2007) 986–988. doi:10.1111/j.1551-2916.2007.01492.x.

[9] X. Mao, S. Shimai, M. Dong, S. Wang, Gelcasting and Pressureless Sintering of Translucent Alumina Ceramics, J. Am. Ceram. Soc. 91 (2008) 1700–1702. doi:10.1111/j.1551-2916.2008.02328.x.

[10] X. Mao, S. Shimai, M. Dong, S. Wang, Investigation of New Epoxy Resins for the Gel Casting of Ceramics, J. Am. Ceram. Soc. 91 (2008) 1354–1356. doi:10.1111/j.1551-2916.2008.02278.x.

[11] R. Xie, K. Zhou, X. Gan, D. Zhang, Effects of Epoxy Resin on Gelcasting Process and Mechanical Properties of Alumina Ceramics, J. Am. Ceram. Soc. 96 (2013) 1107–1112. doi:10.1111/jace.12256.

[12] A. Krell, J. Klimke, Effects of the Homogeneity of Particle Coordination on Solid-State Sintering of Transparent Alumina, J Am Ceram Soc. 89 (2006) 1985–1992.

[13] E.S. Putna, J. Stubenrauch, J.M. Vohs, R.J. Gorte, Ceria-Based Anodes for the Direct Oxidation of Methane in Solid Oxide Fuel Cells, Langmuir. 11 (1995) 4832–4837. doi:10.1021/la00012a040.

[14] H. Inaba, H. Tagawa, Ceria-based solid electrolytes, Solid State Ion. 83 (1996) 1–16.

[15] M. Molenda, K. Furczoń, A. Kochanowski, S. Zapotoczny, M. Szuwarzyński, B. Dudek, R. Dziembaj, Application of gelcasting process in ceria membranes formation, Solid State Ion. 188 (2011) 135–139. doi:10.1016/j.ssi.2010.11.005.

[16] P. Fornasiero, G. Balducci, J. Kašpar, S. Meriani, R. Di Monte, M. Graziani, Metal-loaded CeO2-ZrO2 solid solutions as innovative catalysts for automotive catalytic converters, Catal. Today. 29 (1996) 47–52.

[17] J. Kašpar, P. Fornasiero, M. Graziani, Use of CeO2-based oxides in the three-way catalysis, Catal. Today. 50 (1999) 285–298. doi:10.1016/S0920-5861(98)00510-0.

[18] A. Trovarelli, C. de Leitenburg, M. Boaro, G. Dolcetti, The utilization of ceria in industrial catalysis, Catal. Today. 50 (1999) 353–367. doi:10.1016/S0920-5861(98)00515-X.

[19] E. Mamontov, T. Egami, R. Brezny, M. Koranne, S. Tyagi, Lattice Defects and Oxygen Storage Capacity of Nanocrystalline Ceria and Ceria-Zirconia, J. Phys. Chem. B. 104 (2000) 11110–11116. doi:10.1021/jp0023011.

[20] A. Katelnikovas, P. Vitta, P. Pobedinskas, G. Tamulaitis, A. Žukauskas, J.-E. Jørgensen, A. Kareiva, Photoluminescence in sol–gel-derived YAG:Ce phosphors, J. Cryst. Growth. 304 (2007) 361–368. doi:10.1016/j.jcrysgro.2007.03.006.

[21] L. Truffault, M.-T. Ta, T. Devers, K. Konstantinov, V. Harel, C. Simmonard, C. Andreazza, I.P. Nevirkovets, A. Pineau, O. Veron, J.-P. Blondeau, Application of nanostructured Ca doped CeO2 for ultraviolet filtration, Mater. Res. Bull. 45 (2010) 527–535. doi:10.1016/j.materresbull.2010.02.008.

[22] H.S. Kim, C.Y. Joung, B.H. Lee, J.Y. Oh, Y.H. Koo, P. Heimgartner, Applicability of CeO2 as a surrogate for PuO2 in a MOX fuel development, J. Nucl. Mater. 378 (2008) 98–104. doi:10.1016/j.jnucmat.2008.05.003.

[23] M.C. Stennett, C.L. Corkhill, L.A. Marshall, N.C. Hyatt, Preparation, characterisation and dissolution of a CeO2 analogue for UO2 nuclear fuel, J. Nucl. Mater. 432 (2013) 182–188. doi:10.1016/j.jnucmat.2012.07.038.

[24] D. Horlait, A. Feledziak, F. Lebreton, N. Clavier, D. Prieur, N. Dacheux, T. Delahaye, Dilatometric study of U1−xAmxO2±δ and U1−xCexO2±δ reactive sintering, J. Nucl. Mater. 441 (2013) 40–46. doi:10.1016/j.jnucmat.2013.05.024.

[25] J. Davies, J.G.P. Binner, The role of ammonium polyacrylate in dispersing concentrated alumina suspensions, J. Eur. Ceram. Soc. 20 (2000) 1539–1553. doi:10.1016/S0955-2219(00)00012-1.

[26] T.F. Tadros, Correlation of viscoelastic properties of stable and flocculated suspensions with their interparticle interactions, Adv. Colloid Interface Sci. 68 (1996) 97–200. doi:10.1016/S0001-8686(96)90047-0.

[27] M. Potoczek, E. Zawadzak, Initiator effect on the gelcasting properties of alumina in a system involving low-toxic monomers, Ceram. Int. 30 (2004) 793–799. doi:10.1016/j.ceramint.2003.09.014.

[28] L.A. De Faria, S. Trasatti, The Point of Zero Charge of CeO2, J. Colloid Interface Sci. 167 (1994) 352–357. doi:10.1006/jcis.1994.1370.

[29] S.M. Olhero, E. Lopes, J.M.F. Ferreira, Fabrication of ceramic microneedles – The role of specific interactions between processing additives and the surface of oxide particles in Epoxy Gel Casting, J. Eur. Ceram. Soc. 36 (2016) 4131–4140. doi:10.1016/j.jeurceramsoc.2016.06.035.

[30] S.M. Olhero, L. Garcia-Gancedo, T.W. Button, F.J. Alves, J.M.F. Ferreira, Innovative fabrication of PZT pillar arrays by a colloidal approach, J. Eur. Ceram. Soc. 32 (2012) 1067–1075. doi:10.1016/j.jeurceramsoc.2011.11.016.

[31] M. Potoczek, A catalytic effect of alumina grains onto polymerization rate of methacrylamide-based gelcasting system, Ceram. Int. 32 (2006) 739–744. doi:10.1016/j.ceramint.2005.05.011.

[32] H.M. Wyss, M. Hütter, M. Müller, L.P. Meier, L.J. Gauckler, Quantification of Microstructures in Stable and Gelated Suspensions from Cryo-SEM, J Colloid Interface Sci. 248 (2002) 340–346.

Caption of Figures

Figure 1: Detailed flowchart of gelcasting process.

Figure 2: TEM micrographs of CeO_2 Opaline^{TM} SM2 powder.

Figure 3: Viscosity of CeO_2 aqueous suspensions (30 vol.%) as a function of dispersant amount with or without EGDGE addition (20wt.%) (a), and rheological behaviour of same CeO_2 suspensions at optimum dispersant content (0.50 wt.%) (b).

Figure 4: Zeta potential of CeO_2 aqueous suspensions as a function of pH for different formulations: CeO_2, CeO_2 added with 0.5wt.% of dispersant **(PAA)** and CeO_2 added with 0.5wt.% of dispersant and EGDGE (**Epoxy,** 20wt.%).

Figure 5: Evolution of the apparent viscosity of CeO_2 aqueous suspensions (30 vol.%) with EGDGE addition (20 wt.%) at different temperatures (a). Illustration of t_{idle} determination from $\eta=f(t)$ plot (b) and corresponding Arrhenius plot $ln(t_{idle})=f(1/T)$ (c). Arrhenius plots obtained for various solid loading of CeO_2 suspensions (error bars were not represented) (d).

Figure 6: Comparison between SEM (-10°C, vacuum) micrograph of CeO_2 suspension with solid-loading of 20 vol.% (a) 47 vol.% (b) after rapid cryogenic solidification and ice sublimation. SEM micrograph of CeO_2 compact after gelcasting and debinding (suspension with 47 vol.%) (c) with corresponding mercury porosimetry measurement (d).

Figure 7: Thermal analysis of CeO_2 sample manufactured by gelcasting with 47 vol.% of solid loading. TG/DSC curves of the dried sample (a); Linear shrinkage and linear shrinkage rate as a function of temperature of the debinded sample (b).

Figure 8: View of CeO_2 green compacts manufactured by gelcasting with various solid loading (a). Corresponding linear shrinkage measured at different steps of the process (b)

Figure 9: SEM micrographs of CeO_2 samples manufactured by gelcasting with various solid loading and sintered at 1500°C during 1 h under air.

Figure 10: View of CeO_2 sintered ceramics with complex shape manufactured by gelcasting of suspensions with solid loading of 47 vol.%.

Tables

Table 1: Activation energies for gelling process of pure EGDGE aqueous solution and colloidal CeO_2 suspensions containing EGDGE.

Volume fraction of CeO_2 (%)	**Activation energy E_a ($kJ.mol^{-1}$)**	**R^2 ***
0	66±4	0.993
10	62±4	0.978
20	67±4	0.985
30	57±3	0.983
40	57±3	0.950

** R^2: linear correlation coefficient*

Table 2: Evolution of CeO_2 ceramics relative density (before and after sintering) measured via Archimede's method and grain size after sintering at 1500°C for 1 h determined from SEM micrographs as a function of CeO_2 suspensions solid loading.

Solid loading (vol.%)	**Relative density of green bodies (%)**	**Macroscopic defects**	**Relative density of sintered bodies (%)**	**Grain size G (µm)**
20	48.1	Yes	84.4	2.65 ± 0.15
30	52.3	Yes	92.4	2.96 ± 0.23
40	52.8	No	94.8	3.27 ± 0.31
45	54.3	No	95.8	3.32 ± 0.24
47	54.9	No	96.1	4.07 ± 0.42
50	55.3	Yes	96.1	4.10 ± 0.26

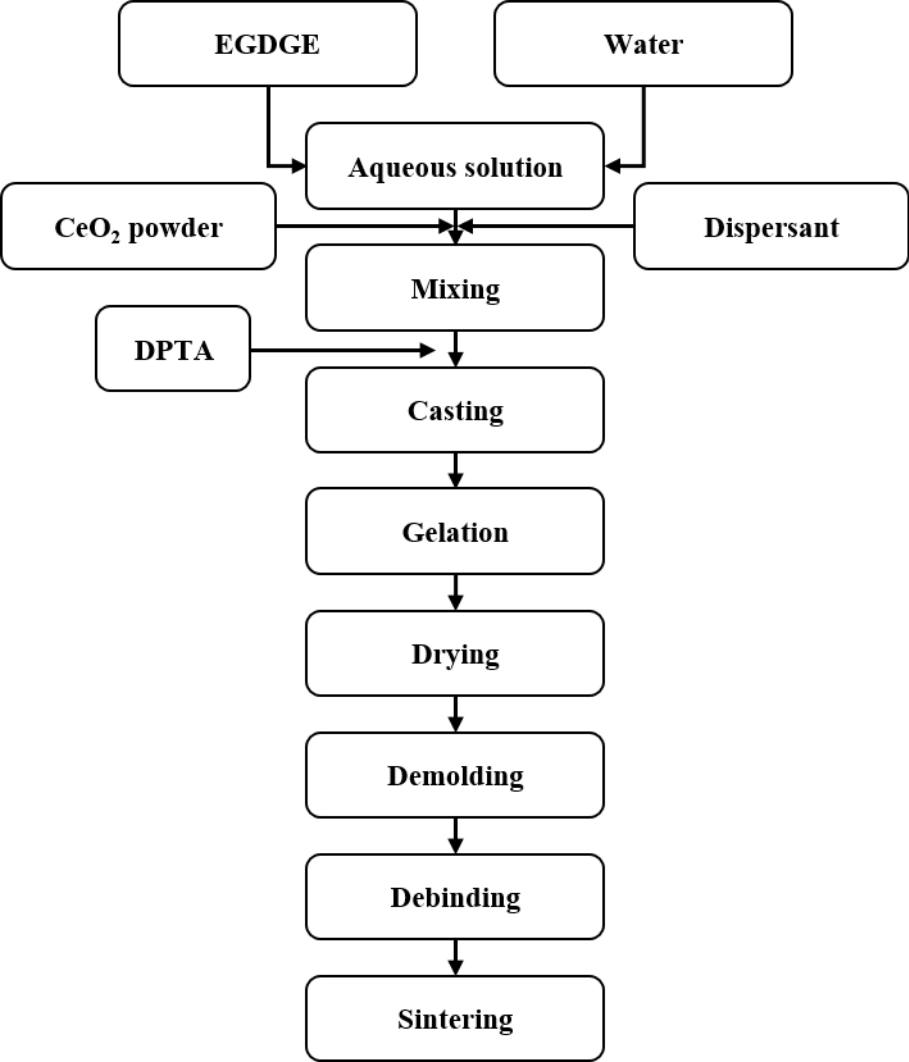
EGDGE
Water
Aqueous solution
CeO_2 powder
Dispersant
Mixing
DPTA
Casting
Gelation
Drying
Demolding
Debinding
Sintering

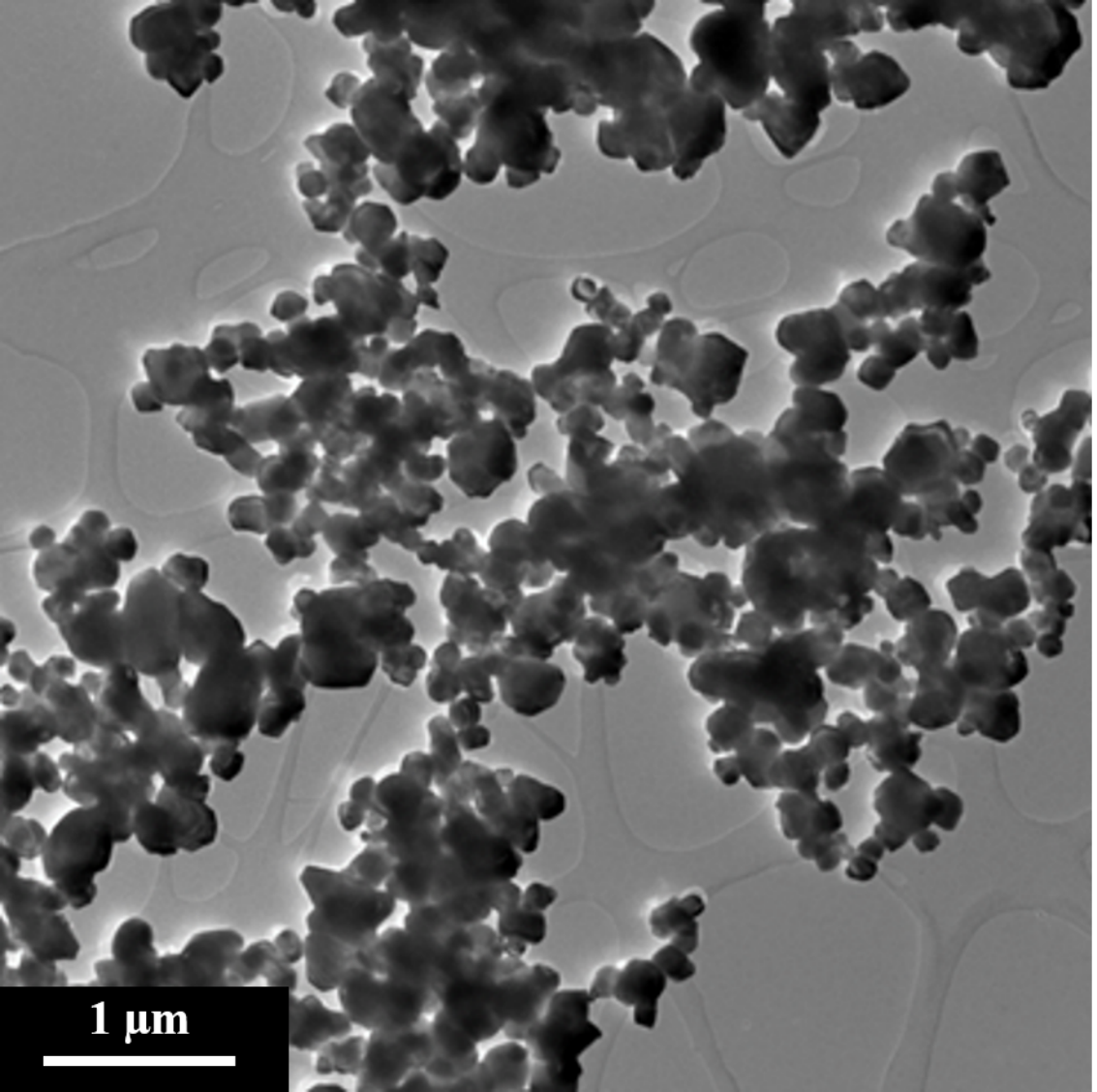
1 µm

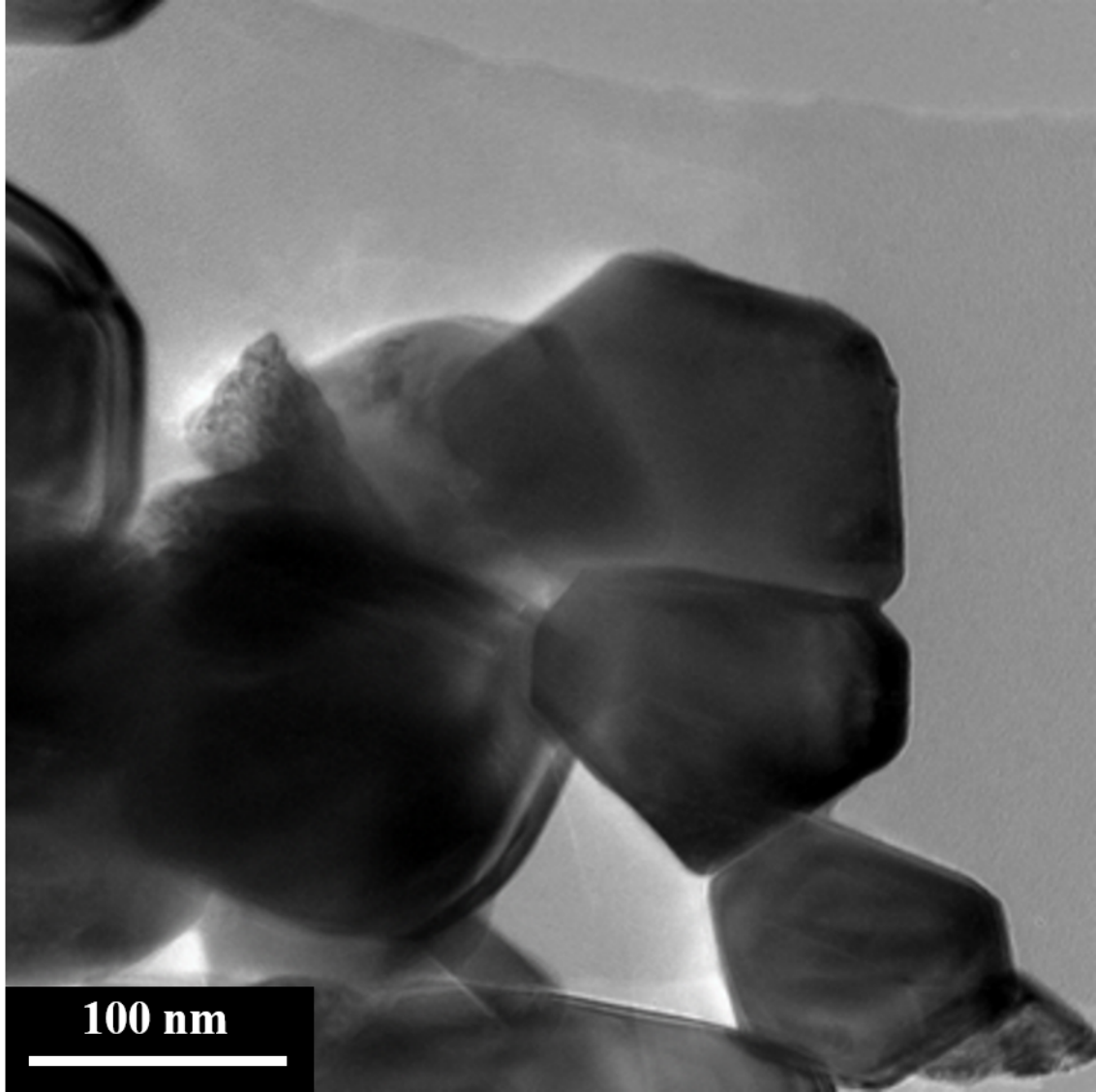
100 nm

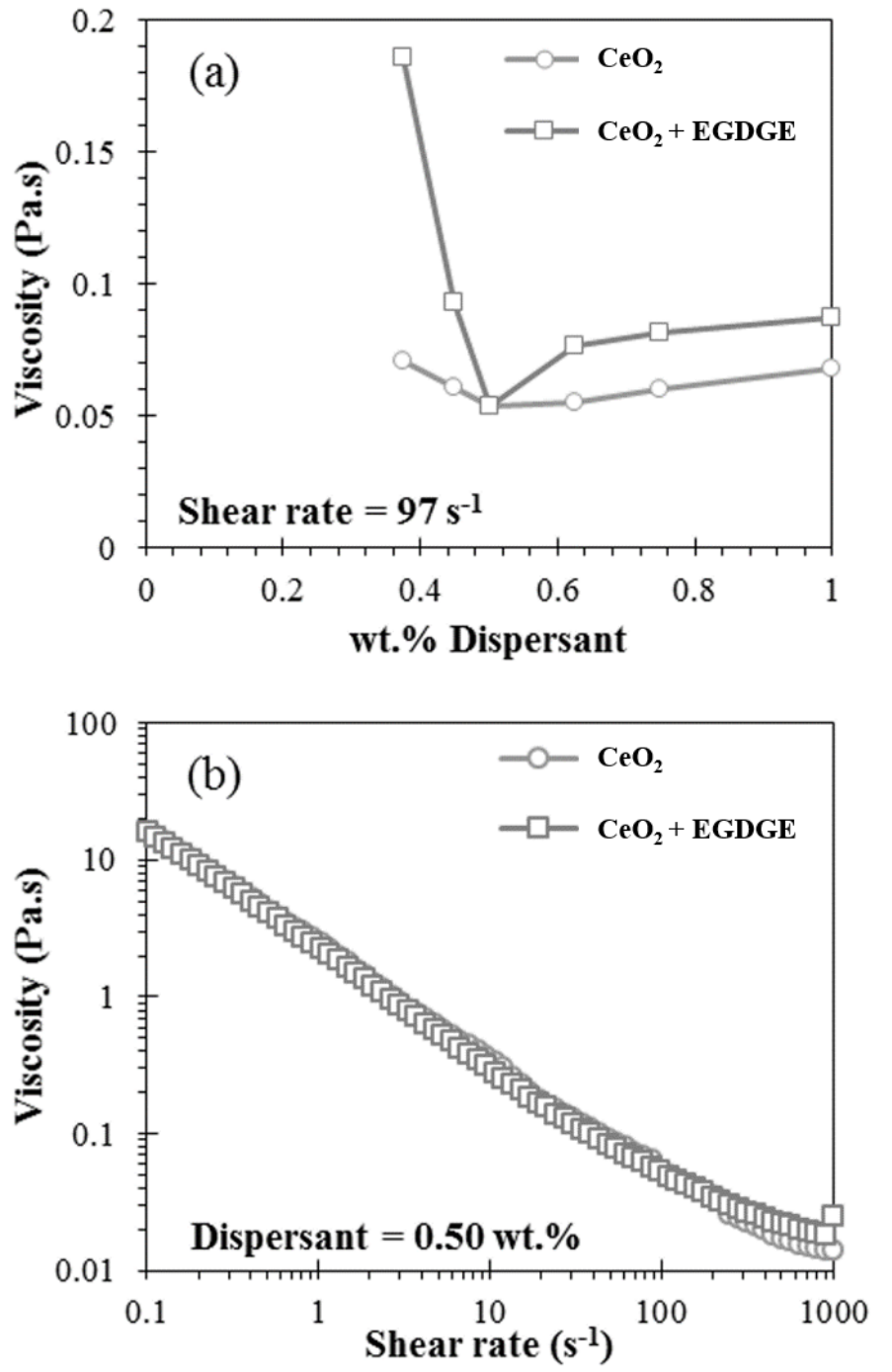
(a)
CeO2
CeO2 + EGDGE
Viscosity (Pa.s)
0.2
0.15
0.1
0.05
0
Shear rate = 97 s-1
0
0.2
0.4
0.6
0.8
1
wt.% Dispersant
(b)
CeO2
CeO2 + EGDGE
Viscosity (Pa.s)
100
10
1
0.1
0.01
Dispersant = 0.50 wt.%
0.1
1
10
100
1000
Shear rate (s-1)

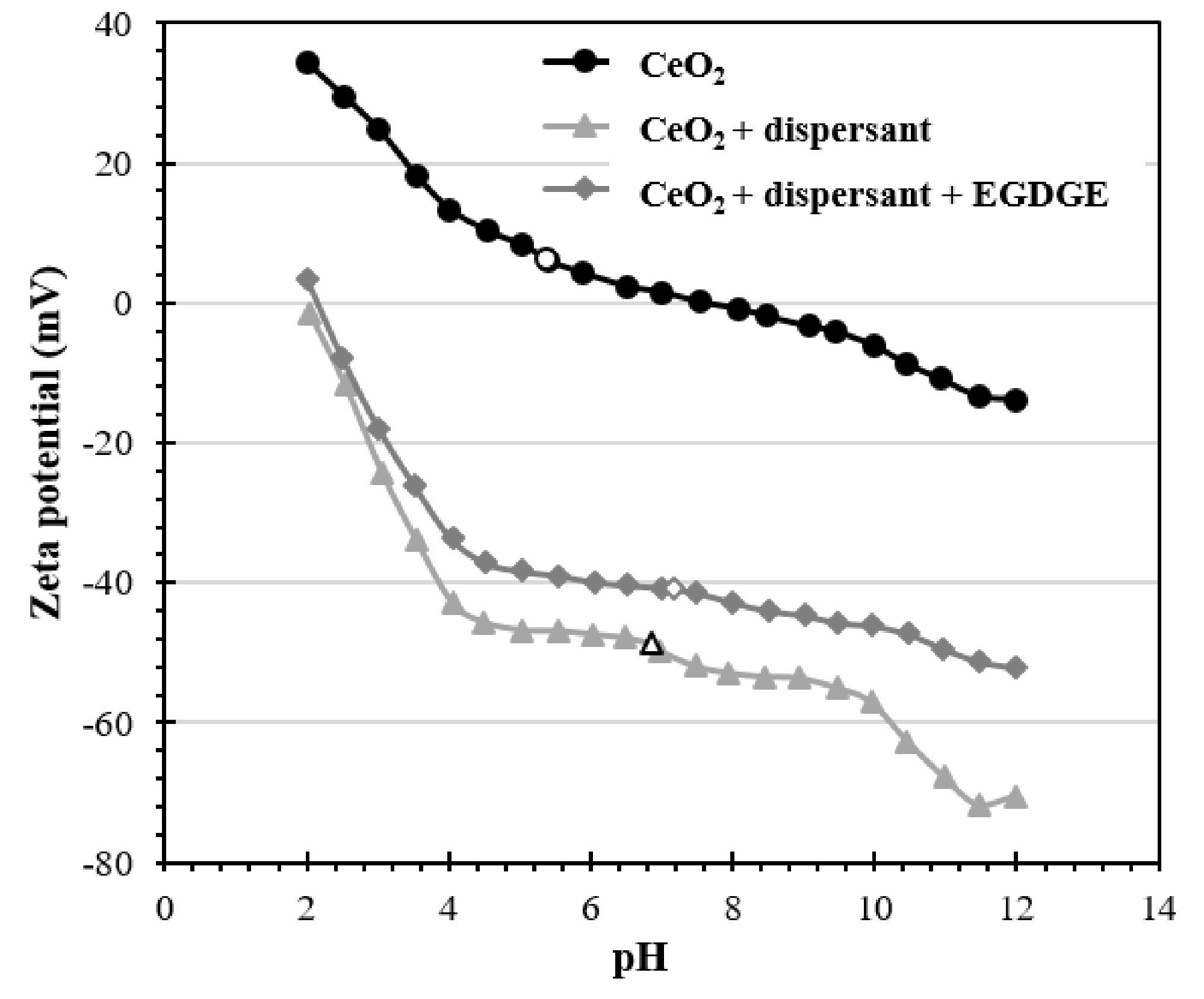
40
20
0
-20
-40
-60
-80
Zeta potential (mV)
0
2
4
6
8
10
12
14
pH
CeO2
CeO2 + dispersant
CeO2 + dispersant + EGDGE

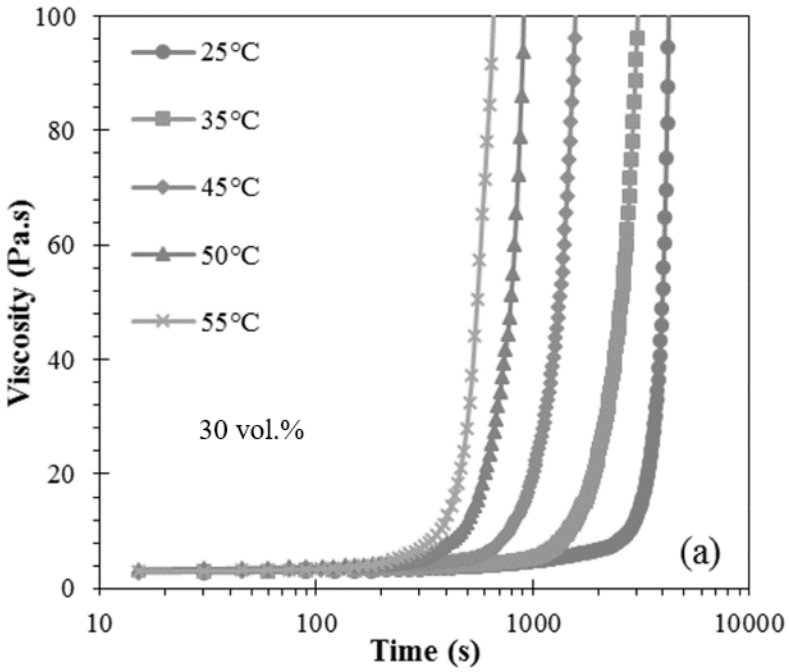
25°C
35°C
45°C
50°C
55°C
30 vol.%
Viscosity (Pa.s)
Time (s)
(a)

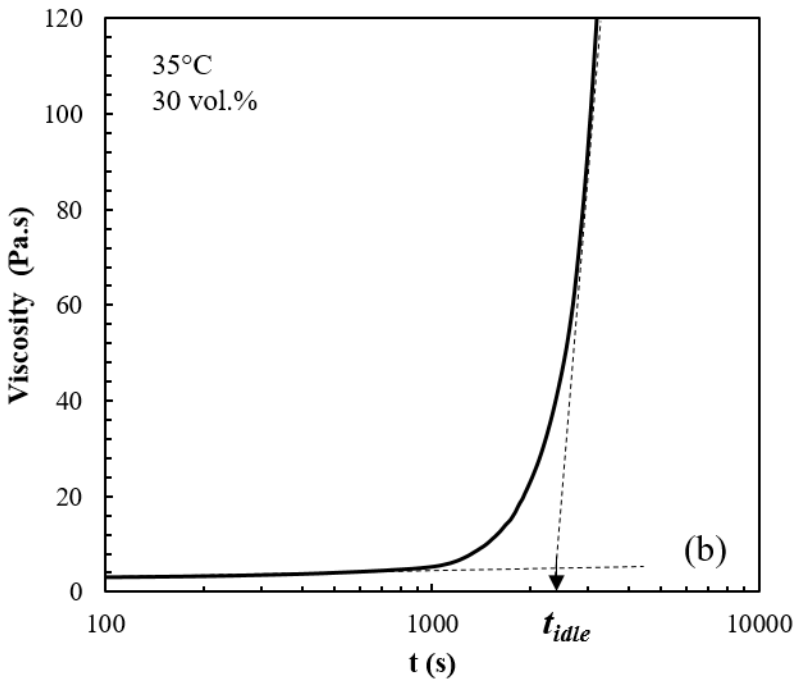
35°C
30 vol.%
Viscosity (Pa.s)
t (s)
t_{idle}
(b)

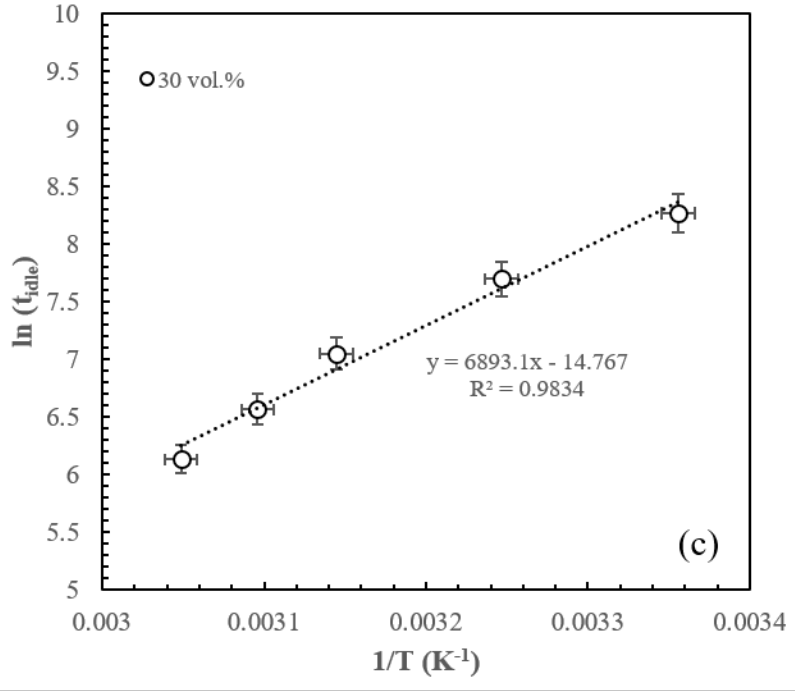
30 vol.%
y = 6893.1x - 14.767
R² = 0.9834
ln (t_{idle})
1/T (K^{-1})
(c)

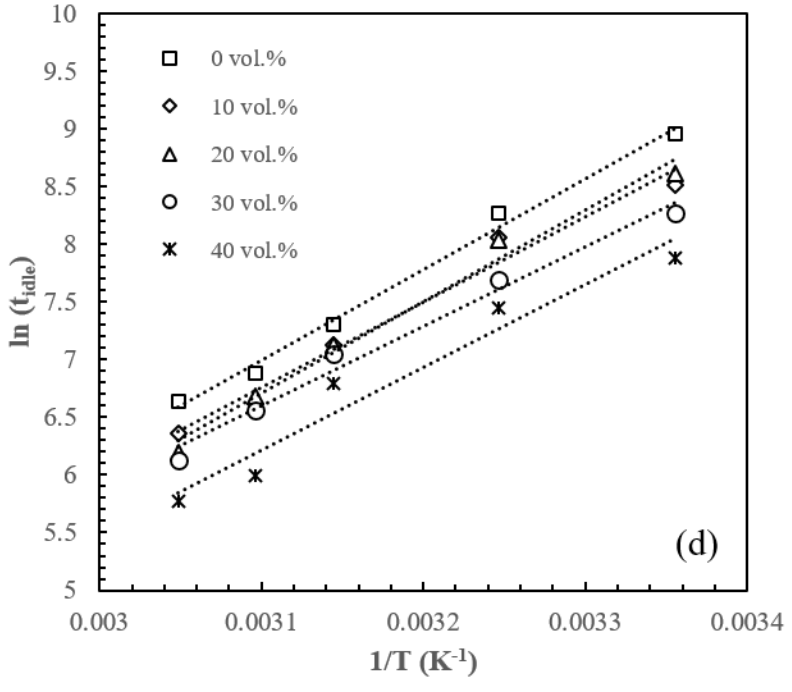
0 vol.%
10 vol.%
20 vol.%
30 vol.%
40 vol.%
ln (t_{idle})
1/T (K^{-1})
(d)

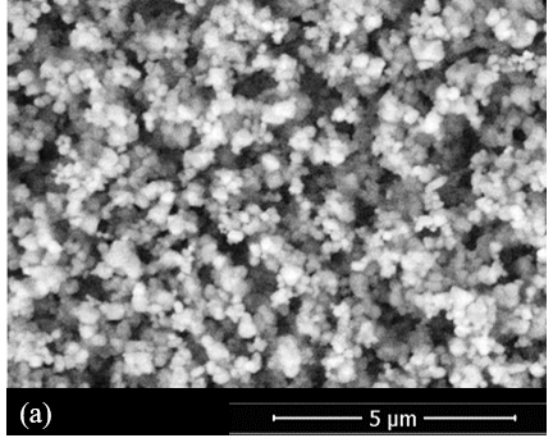
(a)
5 µm

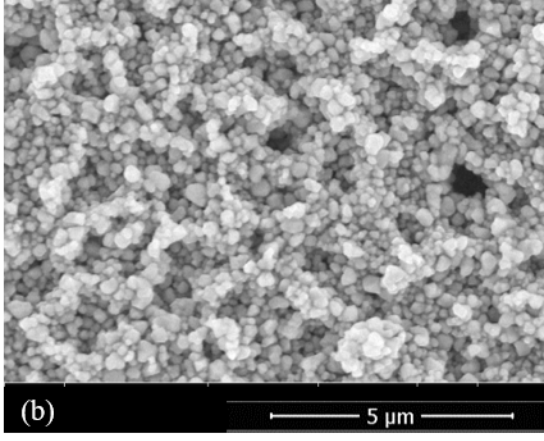
(b)
5 µm

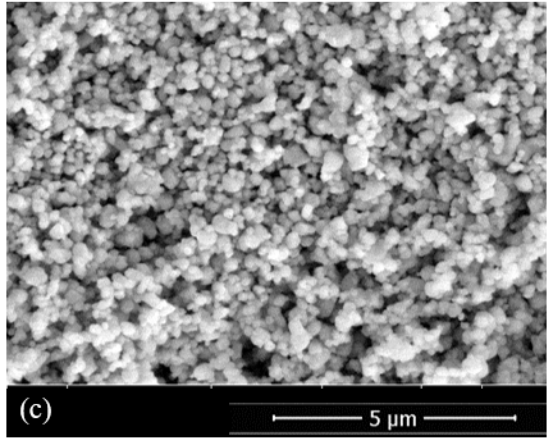
(c)
5 µm

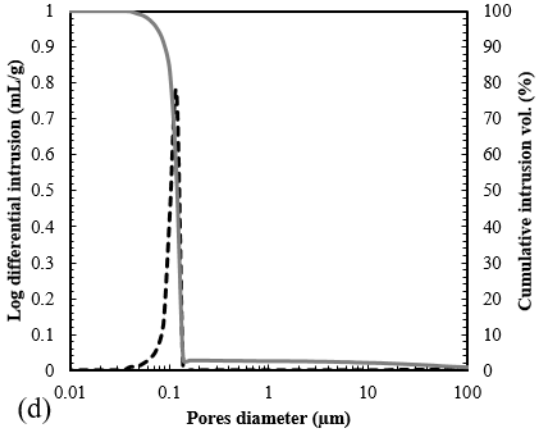
Log differential intrusion (mL/g)
Cumulative intrusion vol. (%)
Pores diameter (µm)
0.01
0.1
1
10
100
(d)

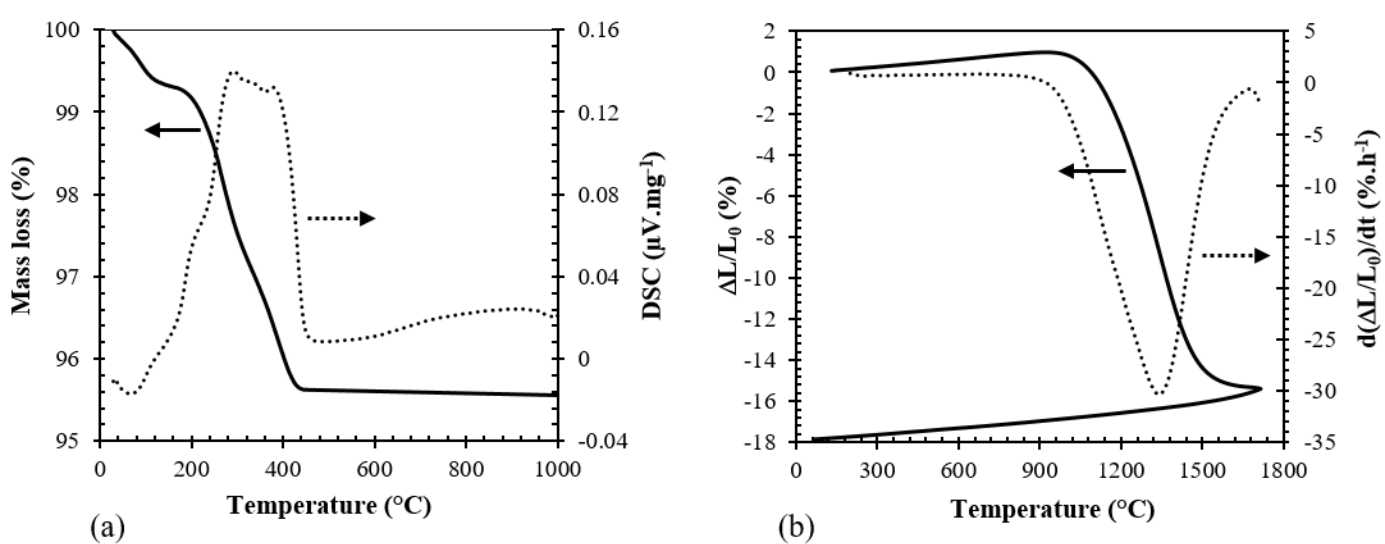
Mass loss (%)
DSC (µV.mg-1)
Temperature (°C)
(a)
ΔL/L0 (%)
d(ΔL/L0)/dt (%.h-1)
Temperature (°C)
(b)

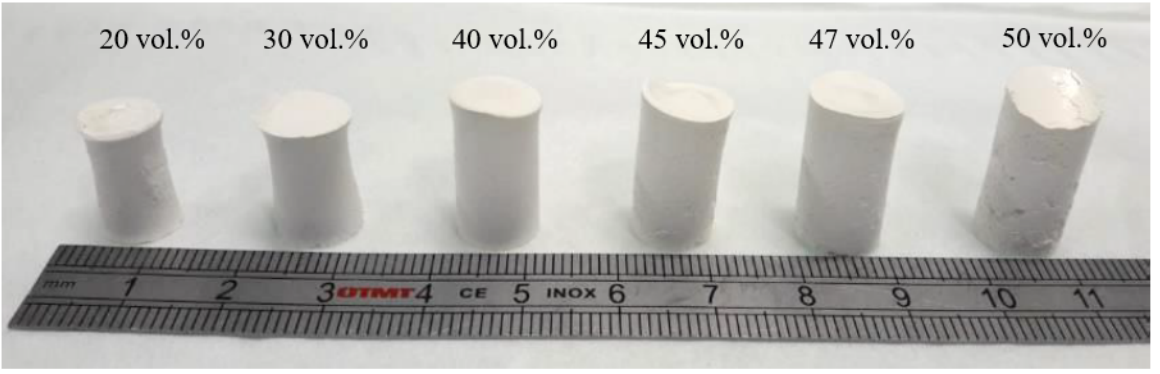
20 vol.%
30 vol.%
40 vol.%
45 vol.%
47 vol.%
50 vol.%
mm
1
2
3
4
5
6
7
8
9
10
11
INOX

(a)

(b)

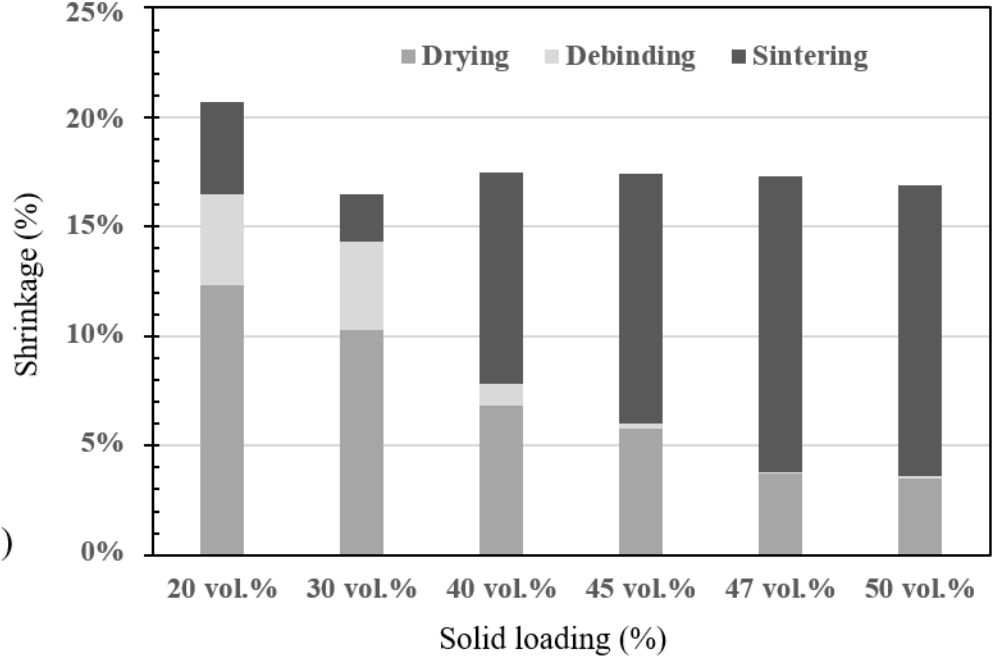
25%
20%
15%
10%
5%
0%
Drying
Debinding
Sintering
Shrinkage (%)
20 vol.%
30 vol.%
40 vol.%
45 vol.%
47 vol.%
50 vol.%
Solid loading (%)

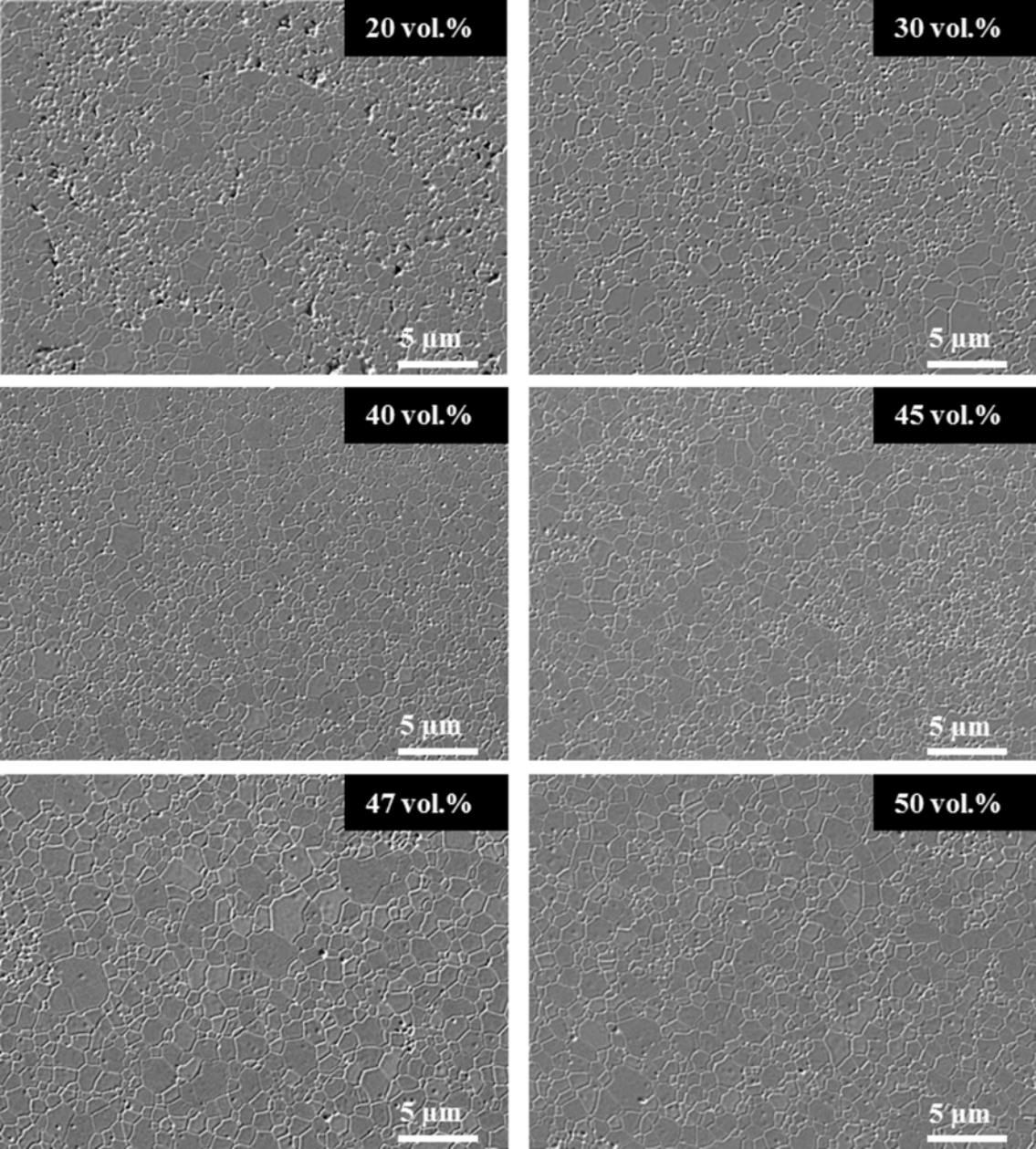
20 vol.%
5 µm
30 vol.%
5 µm
40 vol.%
5 µm
45 vol.%
5 µm
47 vol.%
5 µm
50 vol.%
5 µm

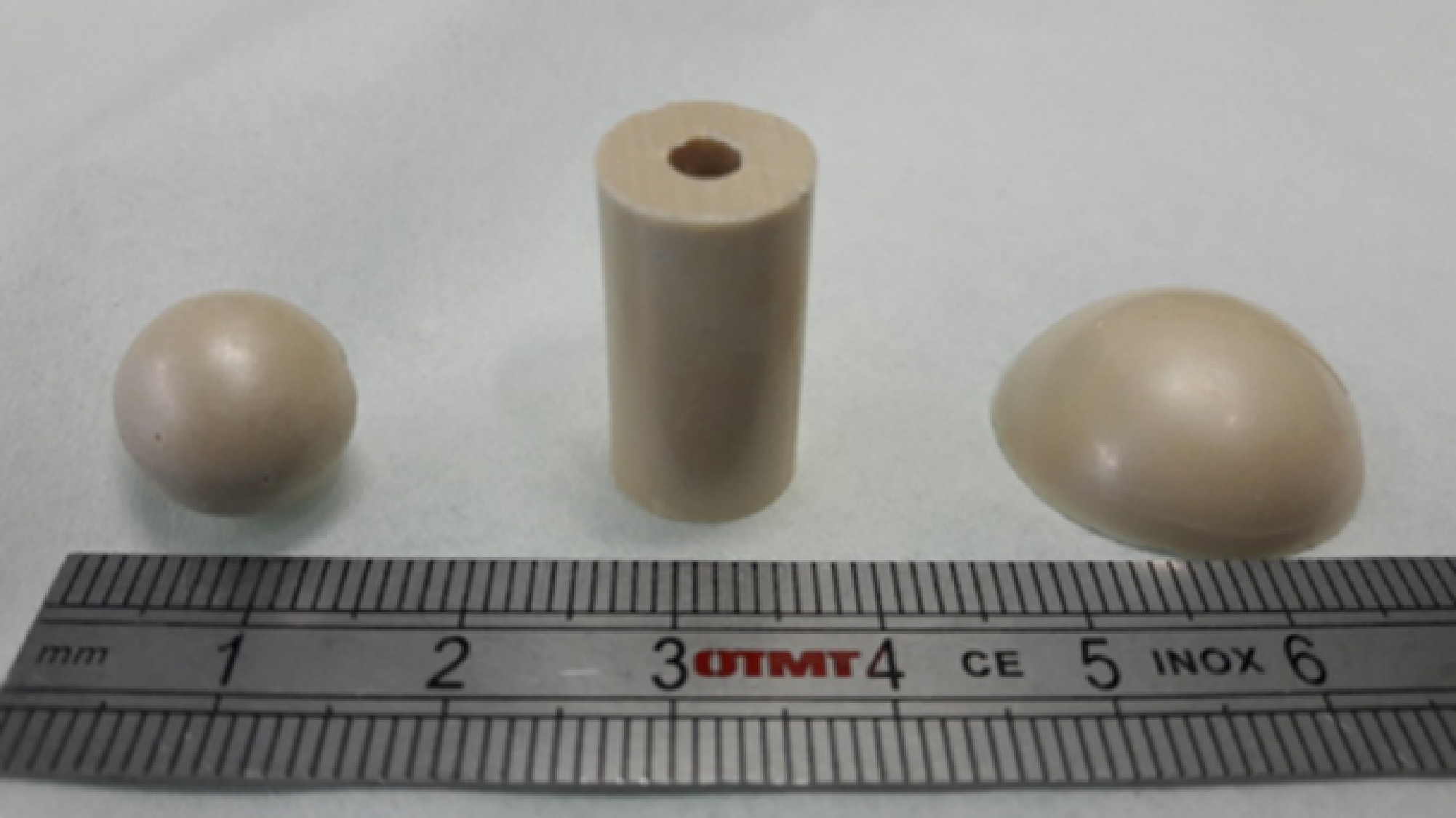
mm
1
2
3
4
5
6
CE
INOX